

Impact of Amino Acid Environment on Electron Attachment to DNA: The Role of Zwitterionic Form

Ankita Gogoi, Jishnu Narayanan S J, Sujan Mandal and Achintya Kumar Dutta*

Department of Chemistry, Indian Institute of Technology Bombay, Powai, Mumbai-400076, India

Abstract

We have studied the effect of zwitterionic form of the amino acid on the electron attachment to DNA using thymine glycine as a model system. The electron attachment to thymine in the presence of glycine takes place through a “doorway mechanism”, where the electron density in the initial anionic state remains away from the nuclear framework of thymine. The electron gets transferred to nucleobase through mixing of electronic and nuclear degrees of freedom and glycine plays an important role in modulating the rate of electron transfer. The charge separation in the zwitterionic glycine make them a better trap for the electron than the native glycine and it can act as a better shield to the incoming electron. However, in the bulk solvated thymine anion the presence of zwitterionic glycine does not lead to any proton transfer to nucleobase, which makes it more resilient to base damage.

*achintya@chem.iitb.ac.in

1. Introduction

The stability of DNA is essential for the survival of living organisms, as alterations in DNA can lead to mutations and subsequent diseases. These alterations include strand breaks, cross-linking between DNA strands or between DNA and proteins, base excision etc. This damage can originate from natural sources, such as reactive oxygen species produced during normal cellular metabolism, or from external agents, particularly radiation. Although cells have efficient repair mechanisms to address DNA damage¹ and maintain genomic stability, their efficiency is compromised in response to radiation-induced DNA damage.²⁻⁴ Soon after the recognition of radiation-induced mutations in 1927⁵, the need to understand the mechanism of biological effects of ionizing radiation gained significant attention. Damage to genetic material can occur via direct, quasi-direct, and indirect action of ionizing radiation.^{2,6} Direct effects occur when ionizing radiation (IR) interacts with DNA and may lead to ionization or excitation.^{2,7-9} Indirect effects result from the interaction of high-energy radiation with surrounding water molecules or proteins. This interaction can either excite or ionize them to form cation radicals and secondary electrons. Both of these species can interact with DNA and induce structural changes.^{10,11} Once generated, secondary electrons undergo inelastic collision with the surrounding aqueous environment, producing low energy electrons (LEEs) with energy ranging from ~0 to 20 eV.¹² As LEEs continue to interact with the surrounding medium, they undergo a sequence of solvation and relaxation processes, eventually becoming thermalized and forming fully solvated electrons (e^-_{aq}) within a picosecond timescale. Along this path, they generate potentially harmful intermediates, such as quasi-free electrons (e^-_{qf}) followed by pre-hydrated electrons (e^-_{pre}), which rapidly undergo solvation within ~500 fs to ultimately yield fully solvated electrons (e^-_{aq}).¹³⁻¹⁶ e^-_{aq} and e^-_{pre} has been shown not to cause strand breaks^{10,17-21}, it is the e^-_{qf} that can cause damage to DNA.

The initial discovery of LEE induced DNA damage²²⁻²⁴ highlighted the crucial role of LEEs in causing radiation-induced damage, prompting extensive experimental^{25,24,26-30} and theoretical³¹⁻³⁹ investigations to understand how LEEs interact with DNA. These studies emphasized on the transient negative ions (TNIs), formed when an incoming free electron is temporarily captured by an unoccupied molecular orbital of a neutral DNA subunit. Such states are resonances, which can decay via autodetachment resulting in the release of extra electron and reverting to the neutral molecule or it may undergo dissociative electron attachment (DEA), leading to bond cleavage and the formation of an anion and a neutral radical.^{40,41} These

resonance states lie energetically above the ground state of the neutral molecule and are therefore characterized by negative vertical electron affinity. Electron attachment to gas-phase DNA subunits can also lead to the formation of bound anionic states, which have positive electron affinities.⁴²⁻⁴⁵ One of the prominent type of bound state observed in DNA is the dipole-bound state, which arises due to charge-dipole interaction.^{46,47} The existence of these dipole-bound states is attributed to the strong dipole moment of DNA. In this case, the excess electron is loosely bound and primarily resides outside the molecular framework.⁴⁵ Another type of bound anionic state is the valence bound one, in which the additional electron density is localized on the molecule and can cause significant alterations in geometry relative to the neutral molecule.^{44,48} Previous reports have shown that the dipole-bound state acts as a doorway for the formation of valence bound states.⁴⁸⁻⁵² Condensed phase simulations on nucleobases and base pairs have also reported this doorway mechanism of electron attachment, where the water-bound state acts as the doorway state.^{51,53-56} Given that the surrounding environment significantly affects the dynamics of electron attachment, it is essential to investigate the role of the medium. In the cellular context, DNA is closely associated with proteins, and hence understanding the influence of neighboring amino acids is crucial to perceive cell response to radiation.

Experiments involving irradiation of DNA with LEEs have revealed that amino acids can play a protective role against radiation damage.^{32,57-64} Solomun and Skalicky reported that protein-bound DNA is less susceptible to LEE-induced damage (~3 eV) than isolated DNA.⁵⁹ Ptasinska et al. attempted to study the role of proteins by exposing a short single-strand DNA, specifically a tetramer (GCAT), to 1 eV electrons in the presence of amino acids (glycine and arginine).⁶⁰ They reported that higher concentrations of amino acids exhibit a protective effect against LEE-induced damage, likely due to van der Waals interactions that shield the DNA molecules. Additionally, gas phase studies on anionic complexes of uracil-glycine, uracil-alanine and thymine-glycine have revealed a barrier-free proton transfer can occur from the carboxylic group of glycine to the nucleobase, stabilizing the excess negative charge localized on it.^{57,58,65} First-principles molecular dynamics simulations confirmed glycine's protective role via proton transfer or electron scavenging.⁶² Amino acids have also been shown to repair guanine radicals.⁶⁶⁻⁶⁸ A DFT study revealed that dehydrogenated guanine anions formed via DEA, can be retrieved to its normal form through a two-electron-coupled proton transfer (TECPT) mechanism.⁶⁷ Recent work by Verma et al.⁵⁵, Wang et al.⁶⁴ and Sarma and coworker⁶⁹ support amino acids' role in mitigating radiation-induced damage to DNA. Most of the previous

studies have used the native form of the amino acid, whereas in biological media amino acid often exists as zwitterionic form.⁷⁰ Micro-solvation studies on TNIs have shown that the zwitterionic glycine can better scavenge the electron density from the nucleobase anion.⁷¹ However, the patterns observed from micro-hydration studies are not often transferable to bulk environment.

Although TNIs are known to play a key role in DNA strand breaks, it is equally important to account for alternative competing pathways. One such pathway involves the formation of a stable π^* -type valence-bound anion, which can suppress strand breaks. Once a base-centered anion is generated, the subsequent transfer of an electron to the dissociative σ^* -type state encounters a considerable kinetic barrier, thereby reducing the likelihood of bond rupture.⁵² In this work, we intend to study the electron-attachment to DNA that results in nucleobase-centered π^* -type valence-bound anion. Due to the large size of DNA, treating the entire molecule using quantum mechanical (QM) methods is computationally expensive. As a result, smaller and more manageable molecular systems are often chosen as model systems to represent specific regions of DNA.⁷² Since the electron density of valence-bound anion is largely localized on nucleobases, they are promising candidates for DNA model systems. Studying nucleobases provides a crucial starting point to unravel the details of this process. Here, thymine is used as a model system for DNA. We have modelled the protein environment of DNA using glycine, since it is the smallest amino acid and therefore minimizes the computational cost. Its isoelectric point is reported to be 6.05. In aqueous solutions at pH 7, it primarily exists in the zwitterionic form. Given that biological environments are largely aqueous and near neutral pH, investigating the effects of zwitterionic glycine on LEE attachment could have important biological implications. The aim of this study is to understand the effect of zwitterionic amino acid on the electron attachment pathways to nucleobases by taking thymine and glycine as a model system.

2. Computational details

To understand the influence of the surrounding environment, we analyzed both microsolvation and bulk solvation effects. For the microsolvation study, we considered a dimer model comprising thymine and a solvent molecule. Specifically, we examined the thymine–water, thymine–neutral glycine, and thymine–zwitterionic glycine complexes. Since multiple interaction sites are possible in the dimer complexes, we performed conformational sampling

using the CREST software⁷³ to generate different conformers. However, the dimer complex with zwitterionic glycine was found to be unstable, as a proton transferred from the ammonium group to the carboxyl group, reverting the structure to its native form. To retain the zwitterionic state, an additional water molecule was added to the thymine-zwitterionic glycine complex, which could stabilize the structure via H-bonding interactions with the charged moieties of zwitterionic glycine. The fifteen lowest energy conformers obtained from CREST were then optimized at the RI-MP2/def2-TZVP level of theory. These conformers were further classified based on the pattern of hydrogen-bonding interactions present. The lowest-energy conformer from each category was selected for further analysis. We have chosen the EA-EOM-DLPNO-CCSD⁷⁴/aug-cc-pVTZ level of theory for evaluating the electron affinity of dimer complexes. The NORMALPNO setting has been used for the EA-EOM-DLPNO-CCSD⁷⁴ calculations. To account for the diffuse nature of the anion wavefunction, 5s, 5p, and 4d diffuse functions were added in an even-tempered manner⁷⁵ to the atom closest to the positive end of the dipole moment vector. Bulk-solvated thymine–solvent systems were then prepared using a CHARMM-compatible force field for thymine and the TIP3P model for water. The topology and parameters for native and zwitterionic glycine were obtained from CHARMM generalized force field (CGenFF) and CHARMM36 MM force field, respectively. The number of molecules required to fill a cubic box of length 40 Å was calculated based on the density of water and glycine at room temperature. Subsequently, three distinct boxes were set up consisting of thymine, 2657 water molecules, 827 native glycine, and 827 zwitterionic glycine molecules respectively. The classical MD simulations were performed with NAMD 2.14.⁷⁶ The non-bonded cutoff distance was set to 12 Å and the system was minimized followed by heating to 300 K with positional constraints on thymine. The thymine-water, thymine-zwitterionic glycine and thymine-native glycine systems were then equilibrated for 1 ns, 10 ns and 20 ns, respectively, under conditions of constant volume and 300 K temperature with periodic boundary conditions. The particle mesh Ewald (PME) technique has been used to account for electrostatic interactions. For the production run, the NPT ensemble was used. A 10 ns production run was performed for thymine-water, 50 ns for thymine-zwitterionic glycine, and 120 ns for thymine-native glycine using a simulation time step of 2 fs. To ensure adequate sampling, the production run was performed three times for each system. The configurations extracted from the production run were then used for the quantum mechanics/molecular mechanics (QM/MM) simulations. To account for the surrounding environment, solvent molecules in the first solvation shell were also included in the QM region along with thymine. The number of molecules was determined by choosing a cut-off distance based on the radial

distribution function plot generated from the classical MD simulations. The chosen cut-offs were 2.7 Å for thymine-water, 2.6 Å for thymine-zwitterionic glycine, 2.8 Å for thymine-native glycine. The molecules in the QM region were treated at the RI-BP86/def2-SVP level of theory and the remaining molecules were treated at the MM level using the same forcefield used in classical MD simulations. The behavior of all three systems was analyzed using QM/MM dynamics in presence of an excess electron. For each system, three QM/MM simulations were conducted for 10 ps with a time step of 0.5 fs. Following the simulations, QM/MM single-point calculations were carried out on snapshots extracted from the QM/MM trajectories using the EA-EOM-DLPNO-CCSD⁷⁴/aug-cc-pVDZ(+5s5p4d) method with a LOOSEPNO setting, maintaining the same QM/MM partition as employed during the QM/MM dynamics. ORCA 5.0.3 has been employed to perform all the QM and QM/MM calculations.⁷⁶⁻⁷⁸

3. Results and Discussion

3.1 Effect of micro solvation

The thymine–glycine complexes generated from conformational sampling were classified into three distinct categories according to their characteristic hydrogen-bonding patterns. These categories were defined based on the specific binding site of glycine on thymine (Figure 1):

1. Glycine interacting with H11 and O7 of thymine.
2. Glycine interacting with H12 and O9 of thymine.
3. Glycine interacting with H12 and O7 of thymine.

This comparative analysis provides valuable insights on how the interaction sites influences the stabilization of the anionic state. For clarity, we denote the three categories of thymine–native glycine conformers as Thy-NGly1, Thy-NGly2, and Thy-NGly3, respectively. Similarly, the corresponding thymine–zwitterionic glycine complexes are labelled as Thy-ZGly1, Thy-ZGly2, and Thy-ZGly3. The optimized structures of Thymine-Native Glycine and Thymine-Zwitterionic Glycine dimer complexes are as shown in Figures 2 and 3, respectively. The left-hand side in both the picture contains the neutral structure and the right-hand side contains the anionic structure. In both Thy-NGly2 and Thy-ZGly2, the carbonyl oxygen (O9) of thymine accepts a proton from glycine in their equilibrium anion geometry. This proton transfer plays a significant role in the stabilization of the anionic state as will be discussed later. In the remaining two categories, a hydrogen-bond exists between the acidic proton of glycine and

thymine O7 atom. Although a proton transfer is not observed here, this hydrogen bond length decreases upon going from neutral to anionic geometry.

Further calculations were carried out to determine vertical electron affinity (VEA), vertical detachment energy (VDE), and adiabatic electron affinity (AEA) for all conformers.

$$\text{VEA} = E_{\text{neutral}} (\text{at neutral geometry}) - E_{\text{anion}} (\text{at neutral geometry})$$

$$\text{VDE} = E_{\text{neutral}} (\text{at anionic geometry}) - E_{\text{anion}} (\text{at anionic geometry})$$

$$\text{AEA} = E_{\text{neutral}} (\text{at neutral geometry}) - E_{\text{anion}} (\text{at anionic geometry})$$

The attachment of electron can lead to the formation of a dipole-bound anion, where the additional electron density is localized away from the geometric framework. As a result, the nuclear geometry of a dipole-bound anion experiences only minimal distortions compared to its neutral precursor. Therefore, we have considered the neutral geometry to represent the dipole-bound anion. The geometric similarity with neutral also causes dipole-bound anions to have nearly identical VEA and AEA.⁷⁹ As shown in Figure 4, the excess electron density in dipole-bound anions, for thymine and monohydrated thymine, is located away from the nuclear framework. The thymine forms a dipole bound anion also in presence of amino acid. The valence-bound anionic states, on the other hand, have the excess electron localized within the nuclear framework, leading to significant geometric distortions, and thus, valence-bound anions are only stable at the anionic geometry. Figures 5 and 6 shows the valence-bound anions of all thymine–glycine complexes under consideration.

Table 1 lists the dipole moment, VEA, VDE, and AEA for thymine and thymine-solvent complexes with water and amino acids, calculated at the EA-EOM-DLPNO-CCSD/aug-cc-pVTZ(+5s5p4d) level of theory. The thymine-water complex exhibits an almost identical VEA compared to isolated thymine, while thymine-glycine complexes show higher VEA values than isolated thymine. On the other hand, Thy-NGly1 is very weakly bound vertically with a VEA of 4 meV, likely due to its relatively low dipole moment (3.18 D). The zwitterionic glycine complex shows higher dipole moment value due to the charge separation. It has been observed before that the correlation between the dipole-moment and VEA of dipole bound states are not often quantitative.⁸⁰ However, overall the zwitterionic forms shows larger VDE's than the native form. The AEA value is found to be positive for the dimer complex of thymine and

glycine where a proton is transferred to thymine from the latter. The thymine-glycine complexes with proton transfer, namely Thy-NGly2 and Thy-ZGly2, also exhibit the highest VDE among all other complexes. It can be inferred that proton transfer from amino acid has a stabilizing effect as reflected in their high AEA and VDE values. Thy-ZGly3 also forms an adiabatically bound anion, although no proton transfer occurs from glycine to thymine. This suggests that the specific site and nature of the hydrogen-bonding interaction also play a crucial role in stabilization of the valence-bound anion.

Two pathways have been recognized for the protective mechanism of amino acids from LEE-induced damage.^{55,62} In the first pathway, amino acids act as a physical shield by directly scavenging the additional electron, thereby preventing its attachment to DNA. The second pathway involves stabilizing the excess negative charge on the nucleobase through favorable interactions or even proton transfer. Figures 5 and 6 illustrates the valence-bound state of all the thymine-glycine complexes, showing that the excess electron is localized on the nucleobase. Hence, although the presence of a single amino acid residue does not lead to physical shielding of thymine from electron attachment in a micro-solvated environment, it can still help in keeping the electron away from the nucleobase framework. The presence of amino acid can form a stable valence-bound anion which can potentially prevent DEA to the genetic material. Additionally, a proton is transferred from glycine to thymine on the valence-bound anion for category 2 complexes. Gutowski and co-workers, based on their photoelectron spectroscopic experiments and DFT calculations⁶⁵ have proposed that an anionic dimer complex of thymine and glycine undergoes a barrier-free proton transfer when the H atom of COOH is coordinated to the O9 atom of thymine. Whereas no proton transfer occurs in complexes with glycine coordinated to the O7 atom of thymine (Figure 1). This difference arises because the excess electron is not localized on the O7 atom, as indicated by the valence-bound state of thymine shown in Figure 4(a). This is consistent with our results where a proton is transferred to the O9 atom in thymine from both native and zwitterionic glycine, thereby forming an adiabatically bound anion. Although, the proton transfer can increase in the stability of valence-bound states, it is not a necessary criterion for the formation of valence bound state. The hydrogen bonding with the O9 atom of thymine can itself provide additional stabilization of the anion. For example, positive AEA value is observed for the Thy-ZGly3 complex, even though no explicit proton transfer from glycine to thymine takes place. In this case, the hydrogen-bonding interaction between the O9 atom and the water molecule at the anionic

geometry (Figure 3(c)) likely stabilizes the excess electron, thereby enabling the formation of an adiabatically bound anion.

Now, the electron attachment induced proton transfer reactions could proceed via two pathways. The first pathway involves a two-step process: where, in the first step a transition from dipole bound to valence bound state occurs, followed by the proton transfer in the second step. The potential energy profile for this mechanism would exhibit two separate energy barriers: one for the transition between the dipole-bound and valence-bound anion without proton transfer. The second one for the proton transfer in the valence bound anion. The second pathway is a concerted electron-proton transfer (CEPT) reaction, where both electron and proton are transferred in a single step without the formation of any intermediate. To investigate the proton transfer mechanism in thymine-glycine complexes, we have calculated the corresponding MEP in the valence-bound anion. If the calculated pathway exhibits a potential energy barrier, it suggests that the proton transfer occurs in a two-step process, where the valence-bound anion acts as an intermediate state. On the other hand, if the pathway is found to be barrierless, it would indicate that both the electron and proton are transferred simultaneously, without the formation of any intermediates, consistent with the CEPT mechanism. To determine the MEP, we performed a Nudged Elastic Band (NEB) calculation at the same level of theory used for optimization. We then recalculated the MEP at the EA-EOM-DLPNO-CCSD/aug-cc-pVTZ(+5s5p4d) level of theory using the intermediate geometries obtained from the NEB calculation. Figure 7 illustrates the MEP between valence bound anion and the final proton transferred product for complexes of thymine with both native and zwitterionic glycine. It can be seen that the proton transfer is a barrierless process, hence, indicating that it is a CEPT reaction.

Previous studies have shown that electron attachment to thymine nucleobase follows a doorway mechanism.⁴⁸ To unravel the impact of microsolvation on dipole-bound to valence-bound transition, we have generated the adiabatic potential energy curve (PEC) of ground and first excited states of anion for isolated thymine and all the dimer complexes considered. This was done by tracing a linear transit from the dipole-bound geometry to the valence-bound geometry. The intermediate geometries along this linear transit were calculated using the following expression:

$$R_{\text{int}} = (1 - \lambda)R_{DB} + R_{VB}$$

where R_{DB} refers to the geometric parameter (bond length, bond angle and dihedral angle) of the dipole bound geometry and R_{VB} represents the corresponding parameters for valence bound geometry. λ varies from 0 to 1 to map the transition between the two states, where $\lambda = 0$ corresponds to the dipole-bound geometry, while $\lambda = 1$ corresponds to the valence-bound geometry.

It can be seen from the figures 8, 9 and 10 that the adiabatic potential energy curve for the ground state and the excited state come close to each other, showing an avoided crossing which indicates strong interaction between the electronic and nuclear motion. The nature of the electronic wavefunction changes rapidly in the vicinity of the avoided crossing region leading to the breakdown of Born Oppenheimer approximation. One can switch to diabatic representation by transforming the adiabatic electronic wavefunctions into diabatic states which retain their character with change in nuclear coordinates and the electron-nuclear coupling is replaced by the electronic coupling between the diabatic states. We have chosen the dipole bound and valence bound states of the anion as the diabatic basis and calculated the coupling between two states by fitting an avoided crossing model potential defined as follows

$$\begin{pmatrix} V_1 & W \\ W & V_2 \end{pmatrix}$$

The off-diagonal term W is assumed to be constant and a fourth-degree polynomial as a function of λ has been used to obtain the diagonal terms V_1 and V_2 .

$$V_i = a\lambda^4 + b\lambda^3 + c\lambda^2 + d\lambda + v_i^0$$

We have evaluated the rate constant using Marcus theory

$$k = \frac{2\pi}{\hbar^2} |W|^2 \sqrt{\frac{1}{4\pi k_B T \lambda_R}} e^{-(\lambda_R + \Delta G^0)^2 / 4\lambda_R k_B T}$$

where λ_R is the reorganization energy, W is the coupling constant and ΔG^0 is the free energy difference between the valence bound and dipole bound states, excluding entropy contribution. Table 2 lists the coupling constants and rate constants for electron transfer in isolated thymine and all complexes of thymine. The rate constant is found to be the highest for thymine–glycine complexes where a proton is transferred from glycine to thymine, namely Thy-NGly2 and Thy-

ZGly2. In these cases, the rate increases by three orders of magnitude relative to isolated thymine. For the other two complexes, where proton transfer does not take place, the rate constant decreases by one order of magnitude in presence of zwitterionic glycine than that observed in the isolated thymine but increases by one order of magnitude with native glycine. This suggests that a proton transfer from both native and zwitterionic glycine enhances the rate of formation of nucleobase-bound anion. As the formation of valence-bound anion becomes more favorable, it may compete with alternative DNA damage pathways, thereby suppressing electron attachment-induced bond cleavage.

However, in the case of Thy-ZGly complexes where proton transfer does not take place, the formation of nucleobase-centered anion is kinetically less favored than isolated thymine. This suggests that the protective effect of amino acids is more pronounced in the presence of native glycine than in a biological environment where glycine exists in its zwitterionic form. Moreover, as proton transfer is strongly dependent on the specific binding site of glycine to thymine, the stability of the resulting anion depends on the interaction geometry. Overall, these observations highlight the significance of site-specific interactions and proton transfer in modulating the protective role of amino acids against electron-induced damage to DNA.

3.2 Effect of bulk solvation

One should exercise caution when extrapolating conclusions about electron attachment to DNA in the cellular environment from microsolvation studies. Thymine-solvent dimer complexes effectively model the solute-solvent interactions. However, they fail to simulate the complexity of the surrounding medium of DNA. The environmental components can substantially impact the behavior of electron attachment by stabilizing the anionic state through their widespread hydrogen bonding network and can affect the energetics and pathways of the process. Therefore, we now consider thymine bulk solvated with amino acid to obtain a complete picture of electron attachment.

As observed in the case of microsolvation, the electron attachment to the nucleobase in the presence of bulk environment involves both ground and excited state of the anion. Figures 11, 12 and 13 present the time evolution of the EA-EOM-DLNO-CCSD dominant transition orbitals corresponding to the first QM/MM trajectories of thymine in bulk water, native glycine and zwitterionic glycine, respectively. In the presence of bulk water, the excess electron density in the ground state is localized on the water molecules initially and the nucleobase

bound state appears as an excited state (See Figure 11). As the simulation progresses, the electron density shifts to the nucleobase forming a stable nucleobase-bound ground state. This transition from solvent-bound to nucleobase-bound state is observed within 2.5 fs and the solvent bound state appears as the first excited state. Previous studies on bulk-solvated uracil and cytosine nucleobases also showed similar results.^{81,54} Likewise, in the presence of native glycine in bulk, a glycine-bound ground state is formed at the beginning and the thymine bound state appears as an excited state (See Figure 12). The thymine-bound state evolves to be the ground state at 13 fs. The electron attachment in the thymine in bulk of zwitterionic glycine follows the same mechanism (See Figure 13). However, in the case of zwitterionic glycine, the transition from solvent-bound to nucleobase-bound state occurs noticeably later, at 27 fs. The charged moieties in zwitterionic glycine are likely to form strong interactions with the excess electron, thereby delaying the scavenging of electron by the nucleobase. Other trajectories also demonstrate similar behavior.

As discussed in the micro-solvation study, interaction of the solvent with the O9 atom of thymine (Figure 1) has a significant role in the stabilization of the anion. Similarly, in bulk solvation, in addition to electron transfer, a proton transfer is also observed in presence of bulk native glycine environment from one of the surrounding solvent molecules to O9 atom of thymine, suggesting a stabilizing effect of glycine. An earlier study on cytosine reports a similar behavior, where a proton is transferred from a nearby glycine molecule in the bulk-solvated environment.⁵⁵ However, the proton transfer process that is involved in the reaction, differs in the three trajectories. In the first trajectory, it is the proton attached to the carbonyl group of glycine that participates in the reaction. The sequence of events for this trajectory is illustrated in Figure 14. The initial proton transfer occurs at around 70 fs, after which the proton returns to the glycine moiety at approximately 800 fs. A subsequent transfer back to the nucleobase takes place near 3 ps, and the proton remains on thymine until the end of the 10 ps simulation. This behavior is also reflected in the evolution of VDE, which will be examined in the following discussion. Similar behavior is observed in the third trajectory. However, in the second trajectory, the proton bonded to the amino group is transferred to the nucleobase. Subsequently, the deprotonation of the amino group is accompanied by an intramolecular proton transfer from the carbonyl group hydrogen to the amino group, thereby restoring its protonated state. This could be attributed to the higher proton affinity of amino group compared to the carbonyl group in glycine.^{82,83} Unlike in the first trajectory, the proton is transferred back

to glycine after ~ 3 ps. No proton transfer occurs for thymine in bulk zwitterionic glycine in any of the snapshots.

To understand the time scale for stabilization of the anion, we also plotted the instantaneous average of vertical detachment energy (VDE) of the ground state of anion for all three trajectories across the three systems as shown in Figure 16. In each case, an initial sharp rise in VDE is observed, indicating a shift of electron density from the solvent to the solute and the gradual stabilization of the nucleobase-bound state. For water, although the transition occurs within <10 fs, the instantaneous average of VDE converges after ~ 1 ps. Similarly in presence of amino acids, although transition happens within a few femtoseconds, the instantaneous average of VDE converges only around ~ 3 ps and ~ 4 ps for thymine-zwitterionic glycine and thymine-native glycine system, respectively. This could possibly be due to the reorientation of solvent molecules around the nucleobase which take time to accommodate the excess electron. This solvent reorganization is faster in water due to the small size of water molecules and hence VDE equilibrates faster as compared to the amino acids. Furthermore, the VDE of the thymine-bound anion is higher in water (~ 4.2 eV) compared to that in amino acids (~ 3.4 eV). A previous study has shown that cytosine-bound anion experiences greater stabilization in bulk water than in native glycine.⁵⁵

In the first trajectory of the thymine-native glycine system, the instantaneous average of the vertical detachment energy (VDE) initially seems to converge to a lower value of ~ 2.6 eV between 700 fs and 2000 fs, suggesting a transient stabilization likely associated with the transferred proton going back to glycine as shown in Figure 14. However, beyond 2000 fs, the VDE begins to increase again, ultimately converging around 4000 fs. This rise in VDE coincides with the proton transfer back to the nucleobase near 3000 fs forming a proton-attached, thymine-bound anion with higher stability. In the remaining two trajectories, the proton is transferred back to glycine once the anion is stabilized. These observations indicate that once a stable thymine-centered bound anion forms after solvent-reorganization, it persists even if the proton subsequently returns to glycine. Such stabilization reduces the availability of secondary electrons that can participate in the formation of transient negative ions (TNIs) which could lead to DNA strand breaks.

It is noteworthy that, while native glycine provides a stronger stabilizing effect than zwitterionic glycine in the microsolvation case, their impact on stabilization of the thymine-centered anion in bulk environment is nearly identical as evident from the VDE of the anion.

Moreover, in the case of bulk-solvated native glycine, proton transfer appears to impact the stabilization of the thymine-centered anion. In contrast, no such proton transfer is observed for zwitterionic glycine across the three trajectories. However, the VDE of the stabilized anion converges to nearly the same value for both amino acid forms. Notably, in aqueous solution, the anion exhibits a relatively higher VDE and reaches equilibration more rapidly, despite the absence of proton transfer. This highlights the crucial role of solvent orientation in bulk environments.

4. Conclusions

In this work, we have studied the role of native and zwitterionic form of the amino acid on the electron attachment process to nucleobases, taking thymine and glycine as a model system. In micro-solvated thymine, in the presence of both the native and zwitterionic forms, the dipole-bound state acts as a doorway. The thymine complexed with zwitterionic form shows a higher dipole moment due to its charge separation, which results in a larger vertical electron affinity value. The magnitude of the adiabatic electron affinity value on the other hand is sensitive to the local geometry and the nature of the hydrogen bonding interactions. In both native and zwitterionic complexes, proton transfer enhances the stability of adiabatically bound valence type state and the proton transfer takes place through a barrierless concerted process. A Marcus estimate of the rate of electron transfer shows that the transfer of electron from dipole bound to valence-bound state can be even faster in some thymine-glycine complexes than that observed in monohydrated thymine.

However, the situation changes in the bulk environment, where the transfer of electron from solvent bound state to solute bound state is much faster in water than in amino acid. The stability of the valence bound state is also highest in aqueous solution. The glycine on the other hand can scavenge the electron and can act as a physical screen between the electron and the nucleobase, thereby reducing the probability of DEA-induced bond breaking. The zwitterionic glycine can have a better shielding effect, as the charge separation delays the electron transfer, and it is less prone to transfer proton to anionic thymine in bulk solvent, which makes it less susceptible to base damage. Although the model system can provide a lot of insights into the role of protein environment in electron attachment induced damage to genetic material, more meaningful model systems including sugar and phosphate group along with the nucleobases and amino acid in polypeptide forms are required. Work in this direction is currently in progress.

Supplementary Material

The optimized geometries of isolated thymine, thymine water, and thymine glycine complex geometry, molecular orbital plots for additional trajectories are provided in the supporting information.

Acknowledgments

The authors gratefully acknowledge financial support from IIT Bombay and the Prime Minister's Research Fellowship. The authors also acknowledge IIT Bombay supercomputing facility and C-DAC supercomputing resources (Param Smriti, Param Brahma, and Param Rudra) for computational time.

References:

- (1) Sancar, A.; Lindsey-Boltz, L. A.; Ünsal-Kaçmaz, K.; Linn, S. Molecular Mechanisms of Mammalian DNA Repair and the DNA Damage Checkpoints. *Annu. Rev. Biochem.* **2004**, *73* (1), 39–85. <https://doi.org/10.1146/annurev.biochem.73.011303.073723>.
- (2) Radiation-Induced Damage in DNA. In *Studies in Physical and Theoretical Chemistry*; Elsevier, 2001; pp 585–622. [https://doi.org/10.1016/s0167-6881\(01\)80023-9](https://doi.org/10.1016/s0167-6881(01)80023-9).
- (3) Sage, E.; Shikazono, N. Radiation-Induced Clustered DNA Lesions: Repair and Mutagenesis. *Free Radical Biology and Medicine* **2017**, *107*, 125–135. <https://doi.org/10.1016/j.freeradbiomed.2016.12.008>.
- (4) Berthel, E.; Ferlazzo, M. L.; Devic, C.; Bourguignon, M.; Foray, N. What Does the History of Research on the Repair of DNA Double-Strand Breaks Tell Us?—A Comprehensive Review of Human Radiosensitivity. *IJMS* **2019**, *20* (21), 5339. <https://doi.org/10.3390/ijms20215339>.
- (5) Muller, H. J. Artificial Transmutation of the Gene. *Science* **1927**, *66* (1699), 84–87. <https://doi.org/10.1126/science.66.1699.84>.
- (6) Narayanan S J, J.; Tripathi, D.; Verma, P.; Adhikary, A.; Dutta, A. K. Secondary Electron Attachment-Induced Radiation Damage to Genetic Materials. *ACS Omega* **2023**, *8* (12), 10669–10689. <https://doi.org/10.1021/acsomega.2c06776>.
- (7) Electron Spin Resonance of Radicals in Irradiated DNA. In *Applications of EPR in Radiation Research*; Springer International Publishing: Cham, 2014; pp 299–352. https://doi.org/10.1007/978-3-319-09216-4_8.
- (8) Ma, J.; Denisov, S. A.; Adhikary, A.; Mostafavi, M. Ultrafast Processes Occurring in Radiolysis of Highly Concentrated Solutions of Nucleosides/Tides. *IJMS* **2019**, *20* (19), 4963. <https://doi.org/10.3390/ijms20194963>.
- (9) Chapter 31. Gamma- and Ion-Beam DNA Radiation Damage: Theory and Experiment. In *Chemical Biology*; Royal Society of Chemistry: Cambridge, 2020; pp 426–457. <https://doi.org/10.1039/9781839162541-00426>.

- (10) Kohanoff, J.; McAllister, M.; Tribello, G. A.; Gu, B. Interactions between Low Energy Electrons and DNA: A Perspective from First-Principles Simulations. *J. Phys.: Condens. Matter* **2017**, *29* (38), 383001. <https://doi.org/10.1088/1361-648x/aa79e3>.
- (11) Wishart, J. F.; Madhava Rao, B. S. *Recent Trends in Radiation Chemistry*; World scientific: Singapore, 2010.
- (12) Alizadeh, E.; Orlando, T. M.; Sanche, L. Biomolecular Damage Induced by Ionizing Radiation: The Direct and Indirect Effects of Low-Energy Electrons on DNA. *Annu. Rev. Phys. Chem.* **2015**, *66* (1), 379–398. <https://doi.org/10.1146/annurev-physchem-040513-103605>.
- (13) Pimblott, S. M.; LaVerne, J. A. On the Radiation Chemical Kinetics of the Precursor to the Hydrated Electron. *J. Phys. Chem. A* **1998**, *102* (17), 2967–2975. <https://doi.org/10.1021/jp980496v>.
- (14) Paik, D. H.; Lee, I.-R.; Yang, D.-S.; Baskin, J. S.; Zewail, A. H. Electrons in Finite-Sized Water Cavities: Hydration Dynamics Observed in Real Time. *Science* **2004**, *306* (5696), 672–675. <https://doi.org/10.1126/science.1102827>.
- (15) Alizadeh, E.; Sanche, L. Precursors of Solvated Electrons in Radiobiological Physics and Chemistry. *Chem. Rev.* **2012**, *112* (11), 5578–5602. <https://doi.org/10.1021/cr300063r>.
- (16) Kumar, A.; Becker, D.; Adhikary, A.; Sevilla, M. D. Reaction of Electrons with DNA: Radiation Damage to Radiosensitization. *IJMS* **2019**, *20* (16), 3998. <https://doi.org/10.3390/ijms20163998>.
- (17) Nabben, F. J.; Karman, J. P.; Loman, H. Inactivation of Biologically Active DNA by Hydrated Electrons. *International Journal of Radiation Biology and Related Studies in Physics, Chemistry and Medicine* **1982**, *42* (1), 23–30. <https://doi.org/10.1080/09553008214550881>.
- (18) K. Kuipers M. V. M. Lafleur, G. Characterization of DNA Damage Induced by Gamma-Radiationderived Water Radicals, Using DNA Repair Enzymes. *International Journal of Radiation Biology* **1998**, *74* (4), 511–519. <https://doi.org/10.1080/095530098141384>.
- (19) Ma, J.; Kumar, A.; Muroya, Y.; Yamashita, S.; Sakurai, T.; Denisov, S. A.; Sevilla, M. D.; Adhikary, A.; Seki, S.; Mostafavi, M. Observation of Dissociative Quasi-Free Electron Attachment to Nucleoside via Excited Anion Radical in Solution. *Nat Commun* **2019**, *10* (1). <https://doi.org/10.1038/s41467-018-08005-z>.
- (20) Ma, J.; Wang, F.; Denisov, S. A.; Adhikary, A.; Mostafavi, M. Reactivity of Prehydrated Electrons toward Nucleobases and Nucleotides in Aqueous Solution. *Sci. Adv.* **2017**, *3* (12). <https://doi.org/10.1126/sciadv.1701669>.
- (21) Kumar, A.; Sevilla, M. D. Role of Excited States in Low-Energy Electron (LEE) Induced Strand Breaks in DNA Model Systems: Influence of Aqueous Environment. *ChemPhysChem* **2009**, *10* (9–10), 1426–1430. <https://doi.org/10.1002/cphc.200900025>.
- (22) Woldhuis, J.; Verberne, J. B.; Lafleur, M. V. M.; Retèl, J.; Blok, J.; Loman, H. γ -Rays Inactivate ϕ X174 DNA in Frozen Anoxic Solutions at -20°C Mainly by Reactions of Dry Electrons. *International Journal of Radiation Biology and Related Studies in Physics, Chemistry and Medicine* **1984**, *46* (4), 329–330. <https://doi.org/10.1080/09553008414551501>.

- (23) Boudaïffa, B.; Cloutier, P.; Hunting, D.; Huels, M. A.; Sanche, L. Resonant Formation of DNA Strand Breaks by Low-Energy (3 to 20 eV) Electrons. *Science* **2000**, *287* (5458), 1658–1660. <https://doi.org/10.1126/science.287.5458.1658>.
- (24) Martin, F.; Burrow, P. D.; Cai, Z.; Cloutier, P.; Hunting, D.; Sanche, L. DNA Strand Breaks Induced by 0–4 eV Electrons: The Role of Shape Resonances. *Phys. Rev. Lett.* **2004**, *93* (6). <https://doi.org/10.1103/physrevlett.93.068101>.
- (25) Huels, M. A.; Boudaïffa, B.; Cloutier, P.; Hunting, D.; Sanche, L. Single, Double, and Multiple Double Strand Breaks Induced in DNA by 3–100 eV Electrons. *J. Am. Chem. Soc.* **2003**, *125* (15), 4467–4477. <https://doi.org/10.1021/ja029527x>.
- (26) Abdoul-Carime, H.; Gohlke, S.; Fischbach, E.; Scheike, J.; Illenberger, E. Thymine Excision from DNA by Subexcitation Electrons. *Chemical Physics Letters* **2004**, *387* (4–6), 267–270. <https://doi.org/10.1016/j.cplett.2004.02.022>.
- (27) Zheng, Y.; Cloutier, P.; Hunting, D. J.; Sanche, L.; Wagner, J. R. Chemical Basis of DNA Sugar–Phosphate Cleavage by Low-Energy Electrons. *J. Am. Chem. Soc.* **2005**, *127* (47), 16592–16598. <https://doi.org/10.1021/ja054129q>.
- (28) Sanche, L. Low Energy Electron-Driven Damage in Biomolecules. *Eur. Phys. J. D* **2005**, *35* (2), 367–390. <https://doi.org/10.1140/epjd/e2005-00206-6>.
- (29) Ptasińska, S.; Denifl, S.; Gohlke, S.; Scheier, P.; Illenberger, E.; Märk, T. D. Decomposition of Thymidine by Low-Energy Electrons: Implications for the Molecular Mechanisms of Single-Strand Breaks in DNA. *Angew Chem Int Ed* **2006**, *45* (12), 1893–1896. <https://doi.org/10.1002/anie.200503930>.
- (30) Zheng, Y.; Cloutier, P.; Hunting, D. J.; Wagner, J. R.; Sanche, L. Phosphodiester and N-Glycosidic Bond Cleavage in DNA Induced by 4–15 eV Electrons. *The Journal of Chemical Physics* **2006**, *124* (6). <https://doi.org/10.1063/1.2166364>.
- (31) Barrios, R.; Skurski, P.; Simons, J. Mechanism for Damage to DNA by Low-Energy Electrons. *J. Phys. Chem. B* **2002**, *106* (33), 7991–7994. <https://doi.org/10.1021/jp013861i>.
- (32) Berdys, J.; Anusiewicz, I.; Skurski, P.; Simons, J. Damage to Model DNA Fragments from Very Low-Energy (<1 eV) Electrons. *J. Am. Chem. Soc.* **2004**, *126* (20), 6441–6447. <https://doi.org/10.1021/ja049876m>.
- (33) Berdys, J.; Skurski, P.; Simons, J. Damage to Model DNA Fragments by 0.25–1.0 eV Electrons Attached to a Thymine Π^* Orbital. *J. Phys. Chem. B* **2004**, *108* (18), 5800–5805. <https://doi.org/10.1021/jp049728i>.
- (34) Anusiewicz, I.; Berdys, J.; Sobczyk, M.; Skurski, P.; Simons, J. Effects of Base π -Stacking on Damage to DNA by Low-Energy Electrons. *J. Phys. Chem. A* **2004**, *108* (51), 11381–11387. <https://doi.org/10.1021/jp047389n>.
- (35) Bao, X.; Wang, J.; Gu, J.; Leszczynski, J. DNA Strand Breaks Induced by Near-Zero-Electronvolt Electron Attachment to Pyrimidine Nucleotides. *Proc. Natl. Acad. Sci. U.S.A.* **2006**, *103* (15), 5658–5663. <https://doi.org/10.1073/pnas.0510406103>.

- (36) Gu, J.; Xie, Y.; Schaefer, H. F. Near 0 eV Electrons Attach to Nucleotides. *J. Am. Chem. Soc.* **2006**, *128* (4), 1250–1252. <https://doi.org/10.1021/ja055615g>.
- (37) Gu, J.; Wang, J.; Leszczynski, J. Electron Attachment-Induced DNA Single Strand Breaks: C₃–O₃ σ-Bond Breaking of Pyrimidine Nucleotides Predominates. *J. Am. Chem. Soc.* **2006**, *128* (29), 9322–9323. <https://doi.org/10.1021/ja063309c>.
- (38) Simons, J. How Do Low-Energy (0.1–2 eV) Electrons Cause DNA-Strand Breaks? *Acc. Chem. Res.* **2006**, *39* (10), 772–779. <https://doi.org/10.1021/ar0680769>.
- (39) Winstead, C.; McKoy, V. Resonant Interactions of Slow Electrons with DNA Constituents. *Radiation Physics and Chemistry* **2008**, *77* (10–12), 1258–1264. <https://doi.org/10.1016/j.radphyschem.2008.05.030>.
- (40) Arumainayagam, C. R.; Lee, H.-L.; Nelson, R. B.; Haines, D. R.; Gunawardane, R. P. Low-Energy Electron-Induced Reactions in Condensed Matter. *Surface Science Reports* **2010**, *65* (1), 1–44. <https://doi.org/10.1016/j.surfrep.2009.09.001>.
- (41) Recent Progress in Dissociative Electron Attachment. In *Advances In Atomic, Molecular, and Optical Physics*; Elsevier, 2017; pp 545–657. <https://doi.org/10.1016/bs.aamop.2017.02.002>.
- (42) Hendricks, J. H.; Lyapustina, S. A.; De Clercq, H. L.; Snodgrass, J. T.; Bowen, K. H. Dipole Bound, Nucleic Acid Base Anions Studied via Negative Ion Photoelectron Spectroscopy. *The Journal of Chemical Physics* **1996**, *104* (19), 7788–7791. <https://doi.org/10.1063/1.471482>.
- (43) Desfrancois, C.; Abdoul-Carime, H.; Schermann, J. P. Electron Attachment to Isolated Nucleic Acid Bases. *The Journal of Chemical Physics* **1996**, *104* (19), 7792–7794. <https://doi.org/10.1063/1.471484>.
- (44) Roca-Sanjuán, D.; Merchán, M.; Serrano-Andrés, L.; Rubio, M. *Ab Initio* Determination of the Electron Affinities of DNA and RNA Nucleobases. *The Journal of Chemical Physics* **2008**, *129* (9), 095104. <https://doi.org/10.1063/1.2958286>.
- (45) Tripathi, D.; Dutta, A. K. Bound Anionic States of DNA and RNA Nucleobases: An EOM-CCSD Investigation. *Int J of Quantum Chemistry* **2019**, *119* (9), e25875. <https://doi.org/10.1002/qua.25875>.
- (46) Lykke, K. R.; Mead, R. D.; Lineberger, W. C. Observation of Dipole-Bound States of Negative Ions. *Phys. Rev. Lett.* **1984**, *52* (25), 2221–2224. <https://doi.org/10.1103/PhysRevLett.52.2221>.
- (47) Crawford, O. H. Negative Ions of Polar Molecules. *Molecular Physics* **1971**, *20* (4), 585–591. <https://doi.org/10.1080/00268977100100561>.
- (48) Tripathi, D.; Dutta, A. K. Electron Attachment to DNA Base Pairs: An Interplay of Dipole- and Valence-Bound States. *J. Phys. Chem. A* **2019**, *123* (46), 10131–10138. <https://doi.org/10.1021/acs.jpca.9b08974>.

- (49) Sommerfeld, T. Coupling between Dipole-Bound and Valence States: The Nitromethane Anion. *Phys. Chem. Chem. Phys.* **2002**, *4* (12), 2511–2516. <https://doi.org/10.1039/b202143a>.
- (50) Sommerfeld, T. Intramolecular Electron Transfer from Dipole-Bound to Valence Orbitals: Uracil and 5-Chlorouracil. *J. Phys. Chem. A* **2004**, *108* (42), 9150–9154. <https://doi.org/10.1021/jp049082u>.
- (51) Mukherjee, M.; Tripathi, D.; Brehm, M.; Riplinger, C.; Dutta, A. K. Efficient EOM-CC-Based Protocol for the Calculation of Electron Affinity of Solvated Nucleobases: Uracil as a Case Study. *J. Chem. Theory Comput.* **2021**, *17* (1), 105–116. <https://doi.org/10.1021/acs.jctc.0c00655>.
- (52) Narayanan S J, J.; Tripathi, D.; Dutta, A. K. Doorway Mechanism for Electron Attachment Induced DNA Strand Breaks. *J. Phys. Chem. Lett.* **2021**, *12* (42), 10380–10387. <https://doi.org/10.1021/acs.jpcclett.1c02735>.
- (53) Mukherjee, M.; Tripathi, D.; Dutta, A. K. Water Mediated Electron Attachment to Nucleobases: Surface-Bound vs Bulk Solvated Electrons. *The Journal of Chemical Physics* **2020**, *153* (4), 044305. <https://doi.org/10.1063/5.0010509>.
- (54) Verma, P.; Ghosh, D.; Dutta, A. K. Electron Attachment to Cytosine: The Role of Water. *J. Phys. Chem. A* **2021**, *125* (22), 4683–4694. <https://doi.org/10.1021/acs.jpca.0c10199>.
- (55) Verma, P.; Narayanan S J, J.; Dutta, A. K. Electron Attachment to DNA: The Protective Role of Amino Acids. *J. Phys. Chem. A* **2023**, *127* (10), 2215–2227. <https://doi.org/10.1021/acs.jpca.2c06624>.
- (56) Narayanan S J, J.; Verma, P.; Adhikary, A.; Kumar Dutta, A. Electron Attachment to the Nucleobase Uracil in Diethylene Glycol: The Signature of a Doorway. *ChemPhysChem* **2024**, *25* (24), e202400581. <https://doi.org/10.1002/cphc.202400581>.
- (57) Gutowski, M.; Dabkowska, I.; Rak, J.; Xu, S.; Nilles, J. M.; Radisic, D.; Bowen Jr, K. H. Barrier-Free Intermolecular Proton Transfer in the Uracil-Glycine Complex Induced by Excess Electron Attachment. *Eur. Phys. J. D* **2002**, *20* (3), 431–439. <https://doi.org/10.1140/epjd/e2002-00168-1>.
- (58) Dąbkowska, I.; Rak, J.; Gutowski, M.; Nilles, J. M.; Stokes, S. T.; Bowen, K. H. Barrier-Free Intermolecular Proton Transfer Induced by Excess Electron Attachment to the Complex of Alanine with Uracil. *The Journal of Chemical Physics* **2004**, *120* (13), 6064–6071. <https://doi.org/10.1063/1.1666042>.
- (59) Solomun, T.; Skalický, T. The Interaction of a Protein–DNA Surface Complex with Low-Energy Electrons. *Chemical Physics Letters* **2008**, *453* (1–3), 101–104. <https://doi.org/10.1016/j.cplett.2007.12.078>.
- (60) Ptasńska, S.; Li, Z.; Mason, N. J.; Sanche, L. Damage to Amino Acid–Nucleotide Pairs Induced by 1 eV Electrons. *Phys. Chem. Chem. Phys.* **2010**, *12* (32), 9367. <https://doi.org/10.1039/b926267a>.
- (61) Szyperska, A.; Gajewicz, A.; Mazurkiewicz, K.; Leszczynski, J.; Rak, J. Theoretical Studies on Interactions between Low Energy Electrons and Protein–DNA Fragments: Valence

Anions of AT-Amino Acids Side Chain Complexes. *Phys. Chem. Chem. Phys.* **2011**, *13* (43), 19499. <https://doi.org/10.1039/c1cp21511f>.

(62) Gu, B.; Smyth, M.; Kohanoff, J. Protection of DNA against Low-Energy Electrons by Amino Acids: A First-Principles Molecular Dynamics Study. *Phys. Chem. Chem. Phys.* **2014**, *16* (44), 24350–24358. <https://doi.org/10.1039/C4CP03906H>.

(63) Wityk, P.; Piątek, R.; Nowak, R.; Kostrzewa-Nowak, D. Generation and Characterization of a DNA-GCN4 Oligonucleotide-Peptide Conjugate: The Impact DNA/Protein Interactions on the Sensitization of DNA. *Molecules* **2020**, *25* (16), 3630. <https://doi.org/10.3390/molecules25163630>.

(64) Wang, X.; Liao, H.; Liu, W.; Shao, Y.; Zheng, Y.; Sanche, L. DNA Protection against Damages Induced by Low-Energy Electrons: Absolute Cross Sections for Arginine–DNA Complexes. *J. Phys. Chem. Lett.* **2023**, *14* (24), 5674–5680. <https://doi.org/10.1021/acs.jpcclett.3c01041>.

(65) Dąbkowska, I.; Rak, J.; Gutowski, M.; Nilles, J. M.; Stokes, S. T.; Radisic, D.; Bowen Jr., K. H. Barrier-Free Proton Transfer in Anionic Complex of Thymine with Glycine. *Phys. Chem. Chem. Phys.* **2004**, *6* (17), 4351–4357. <https://doi.org/10.1039/B406455K>.

(66) Milligan, J. R.; Tran, N. Q.; Ly, A.; Ward, J. F. Peptide Repair of Oxidative DNA Damage. *Biochemistry* **2004**, *43* (17), 5102–5108. <https://doi.org/10.1021/bi030232l>.

(67) Jena, N. R.; Mishra, P. C.; Suhai, S. Protection Against Radiation-Induced DNA Damage by Amino Acids: A DFT Study. *J. Phys. Chem. B* **2009**, *113* (16), 5633–5644. <https://doi.org/10.1021/jp810468m>.

(68) Alvarez-Idaboy, J. R.; Galano, A. On the Chemical Repair of DNA Radicals by Glutathione: Hydrogen vs Electron Transfer. *J. Phys. Chem. B* **2012**, *116* (31), 9316–9325. <https://doi.org/10.1021/jp303116n>.

(69) Sarmah, M. P.; Medhi, B.; Sarma, M. Impact of the Electron Attachment to the Alanine Glycine and Glycyl Alanine Conformers. *The Journal of Chemical Physics* **2026**, *164* (5), 054307. <https://doi.org/10.1063/5.0297297>.

(70) Marchese, R.; Grandori, R.; Carloni, P.; Raugeri, S. On the Zwitterionic Nature of Gas-Phase Peptides and Protein Ions. *PLoS Comput Biol* **2010**, *6* (5), e1000775. <https://doi.org/10.1371/journal.pcbi.1000775>.

(71) Arora, S.; Narayanan S J, J.; Haritan, I.; Adhikary, A.; Dutta, A. K. Effect of Protein Environment on the Shape Resonances of RNA Pyrimidine Nucleobases: Insights from a Model System. *The Journal of Chemical Physics* **2025**, *163* (13), 134103. <https://doi.org/10.1063/5.0288514>.

(72) Gu, J.; Leszczynski, J.; Schaefer, H. F. Interactions of Electrons with Bare and Hydrated Biomolecules: From Nucleic Acid Bases to DNA Segments. *Chem. Rev.* **2012**, *112* (11), 5603–5640. <https://doi.org/10.1021/cr3000219>.

(73) Pracht, P.; Bohle, F.; Grimme, S. Automated Exploration of the Low-Energy Chemical Space with Fast Quantum Chemical Methods. *Phys. Chem. Chem. Phys.* **2020**, *22* (14), 7169–7192. <https://doi.org/10.1039/C9CP06869D>.

- (74) Dutta, A. K.; Saitow, M.; Demoulin, B.; Neese, F.; Izsák, R. A Domain-Based Local Pair Natural Orbital Implementation of the Equation of Motion Coupled Cluster Method for Electron Attached States. *The Journal of Chemical Physics* **2019**, *150* (16), 164123. <https://doi.org/10.1063/1.5089637>.
- (75) Tripathi, D.; Dutta, A. K. Bound Anionic States of DNA and RNA Nucleobases: An EOM-CCSD Investigation. *Int J of Quantum Chemistry* **2019**, *119* (9), e25875. <https://doi.org/10.1002/qua.25875>.
- (76) Phillips, J. C.; Braun, R.; Wang, W.; Gumbart, J.; Tajkhorshid, E.; Villa, E.; Chipot, C.; Skeel, R. D.; Kalé, L.; Schulten, K. Scalable Molecular Dynamics with NAMD. *J Comput Chem* **2005**, *26* (16), 1781–1802. <https://doi.org/10.1002/jcc.20289>.
- (77) Neese, F.; Wennmohs, F.; Becker, U.; Riplinger, C. The ORCA Quantum Chemistry Program Package. *The Journal of Chemical Physics* **2020**, *152* (22), 224108. <https://doi.org/10.1063/5.0004608>.
- (78) Neese, F. Software Update: The ORCA Program System—Version 5.0. *WIREs Comput Mol Sci* **2022**, *12* (5), e1606. <https://doi.org/10.1002/wcms.1606>.
- (79) Svozil, D.; Frigato, T.; Havlas, Z.; Jungwirth, P. Ab Initio Electronic Structure of Thymine Anions. *Phys. Chem. Chem. Phys.* **2005**, *7* (5), 840. <https://doi.org/10.1039/b415007d>.
- (80) Tripathi, D.; Dutta, A. K. Bound Anionic States of DNA and RNA Nucleobases: An EOM-CCSD Investigation. *Int J of Quantum Chemistry* **2019**, *119* (9), e25875. <https://doi.org/10.1002/qua.25875>.
- (81) Mukherjee, M.; Tripathi, D.; Dutta, A. K. Water Mediated Electron Attachment to Nucleobases: Surface-Bound vs Bulk Solvated Electrons. *The Journal of Chemical Physics* **2020**, *153* (4), 044305. <https://doi.org/10.1063/5.0010509>.
- (82) Yu, D.; Rauk, A.; Armstrong, D. A. Radicals and Ions of Glycine: An Ab Initio Study of the Structures and Gas-Phase Thermochemistry. *J. Am. Chem. Soc.* **1995**, *117* (6), 1789–1796. <https://doi.org/10.1021/ja00111a017>.
- (83) Nacsa, A. B.; Czakó, G. Benchmark *Ab Initio* Proton Affinity of Glycine. *Phys. Chem. Chem. Phys.* **2021**, *23* (16), 9663–9671. <https://doi.org/10.1039/D1CP00376C>.

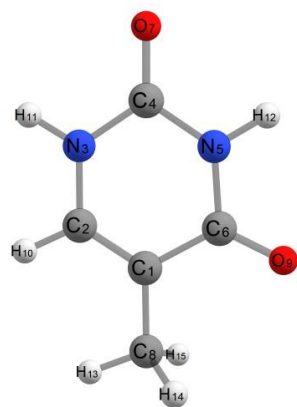


Figure 1. Optimized structure of thymine at neutral geometry.

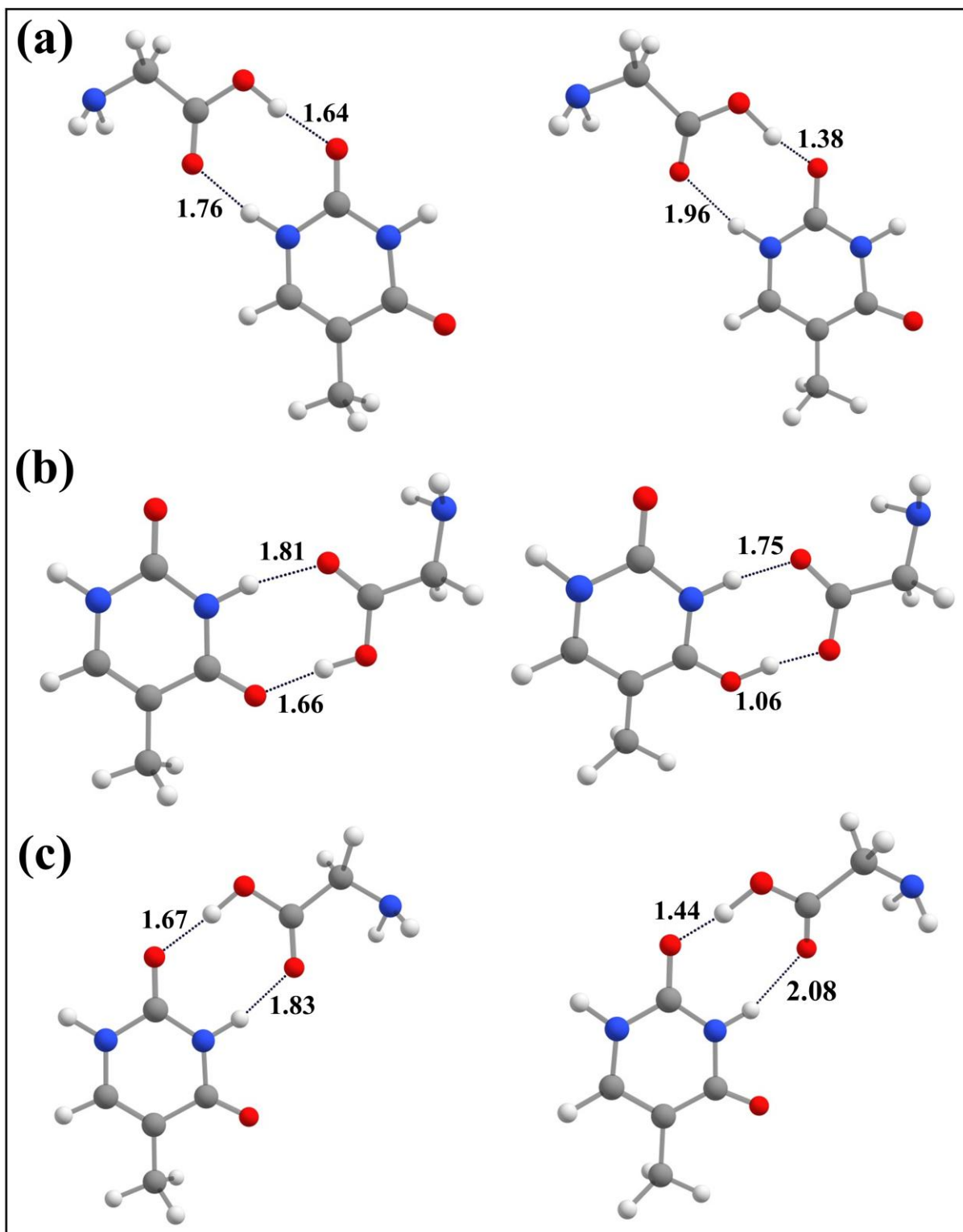


Figure 2. Optimized structures for (a) Thy-NGly1 (b)Thy-NGly2 and (c) Thy-NGly3 at neutral (left) and anionic (right) geometry.

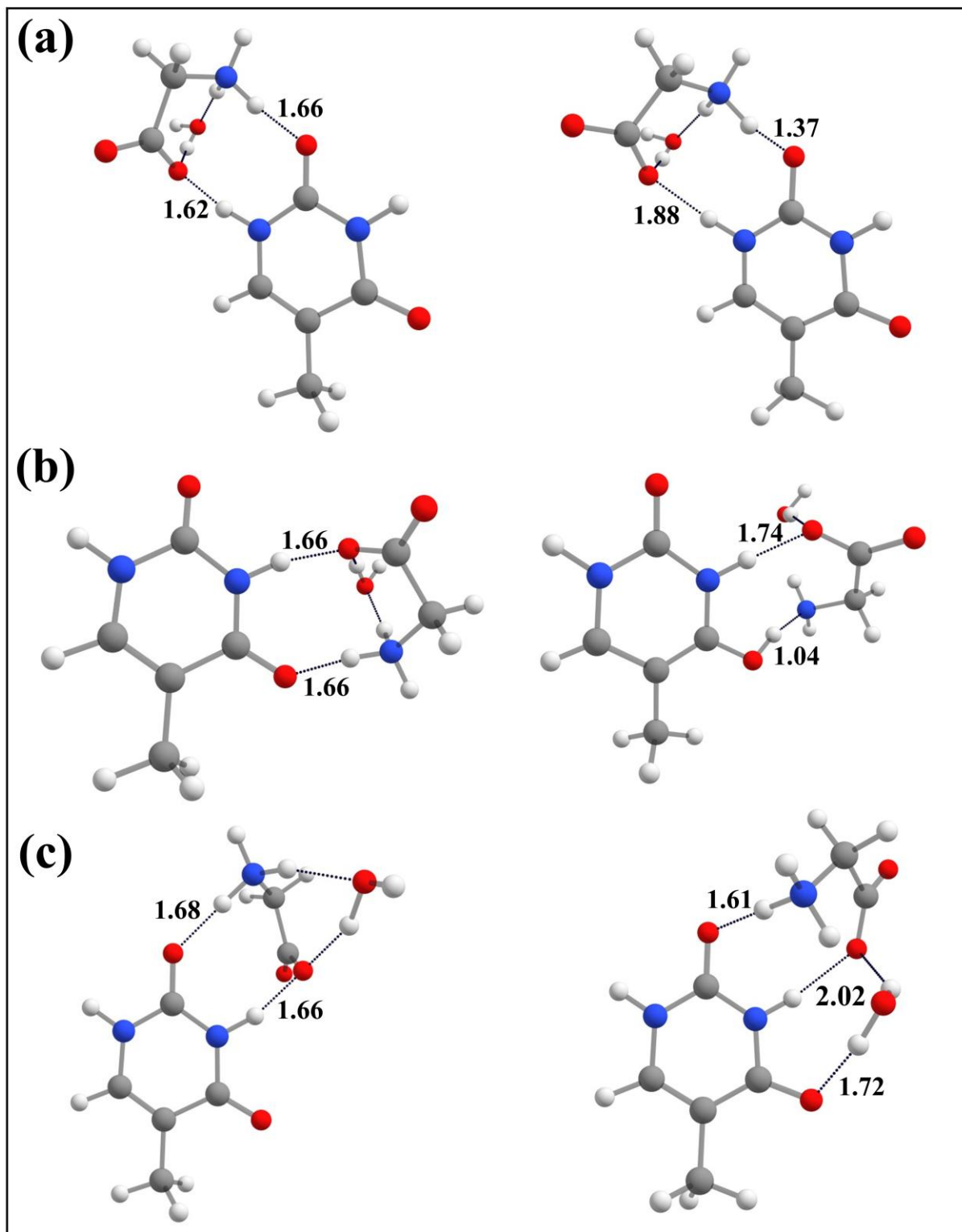


Figure 3. Optimized structures for (a) Thy-ZGly1 (b)Thy-ZGly2 and (c) Thy-ZGly3 at neutral (left) and anionic (right) geometry.

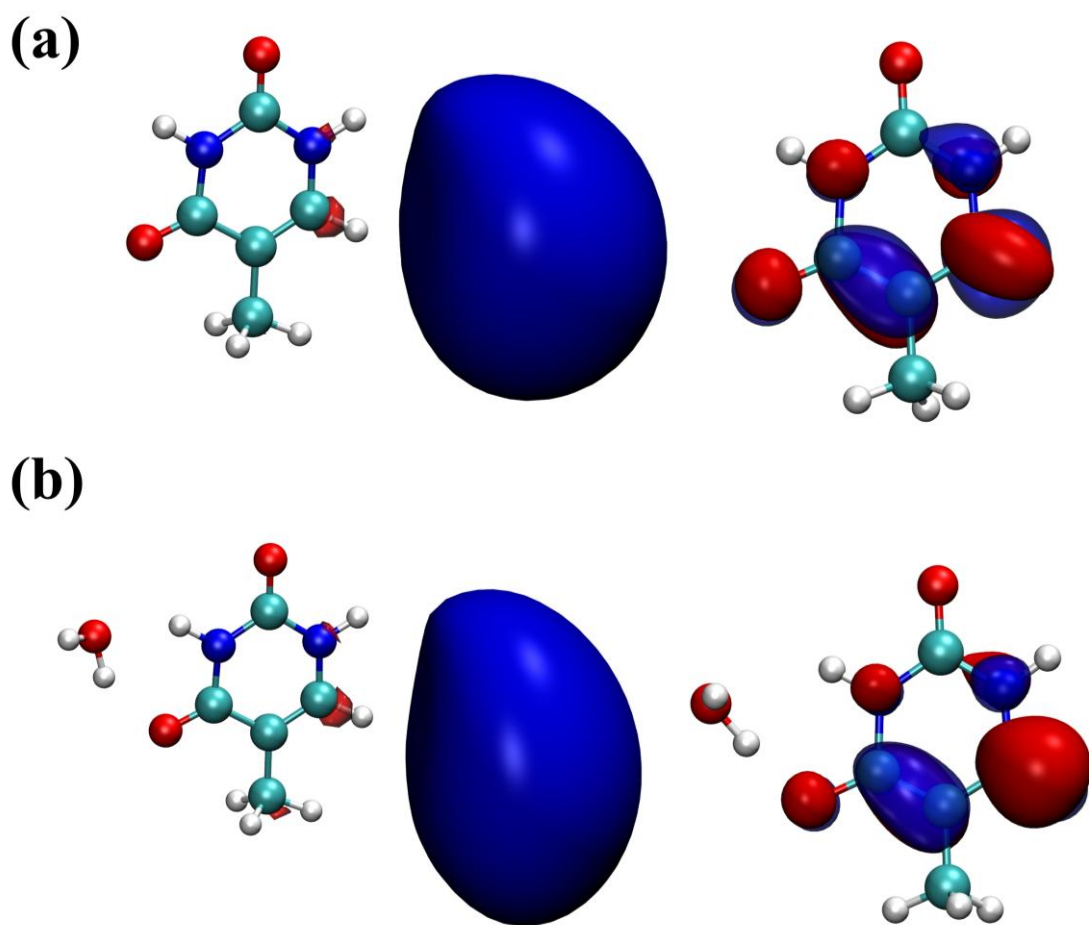


Figure 4. Natural orbitals corresponding to the dipole bound anions (left) and valence bound anions (right) for (a) isolated-thymine and (b) thymine-water.

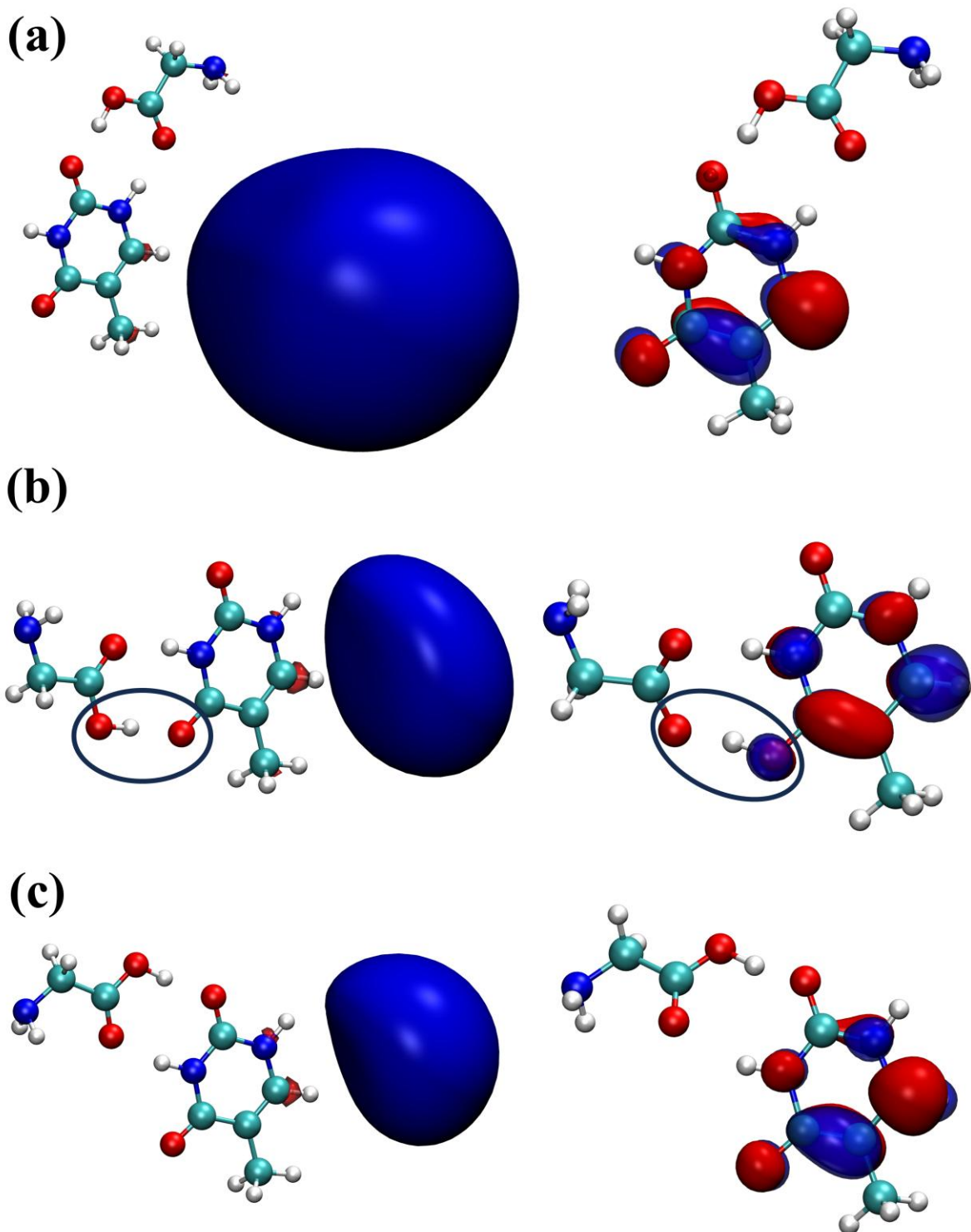


Figure 5. Natural orbitals corresponding to the dipole bound anions (left) and valence bound anions (right) for (a)Thy-NGly1, (b) Thy-NGly2, (c)Thy-NGly3.

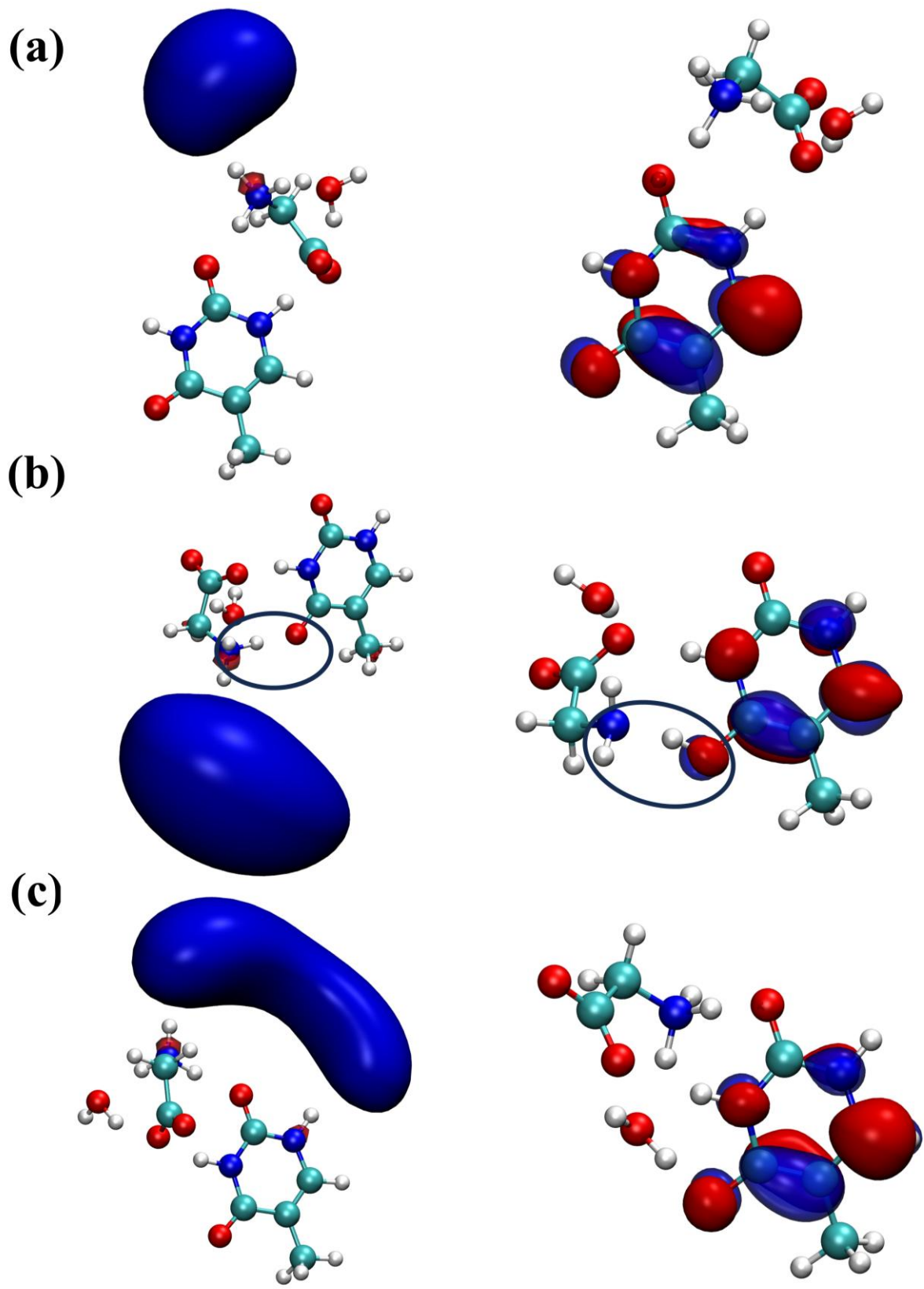


Figure 6. Natural orbitals corresponding to the dipole bound anions (left) and valence bound anions (right) for (a)Thy-ZGly1, (b) Thy-ZGly2, (c)Thy-ZGly3.

Table 1. Dipole moment (in Debye) and VEA, VDE and AEA (all values are in meV) of Isolated Thymine, Thymine-Water and Thymine-Glycine Complexes.

Complex	Dipole moment	VEA	VDE	AEA
Isolated thymine	4.88	48	570	-231
Thymine-Water	4.95	40	937	-4
Thy-NGly ₁	3.18	4	862	-90
Thy-NGly ₂	6.05	65	1883	300
Thy-NGly ₃	6.15	74	865	-103
Thy-ZGly ₁	6.04	127	890	-109
Thy-ZGly ₂	8.70	77	2125	563
Thy-ZGly ₃	10.30	132	1456	315

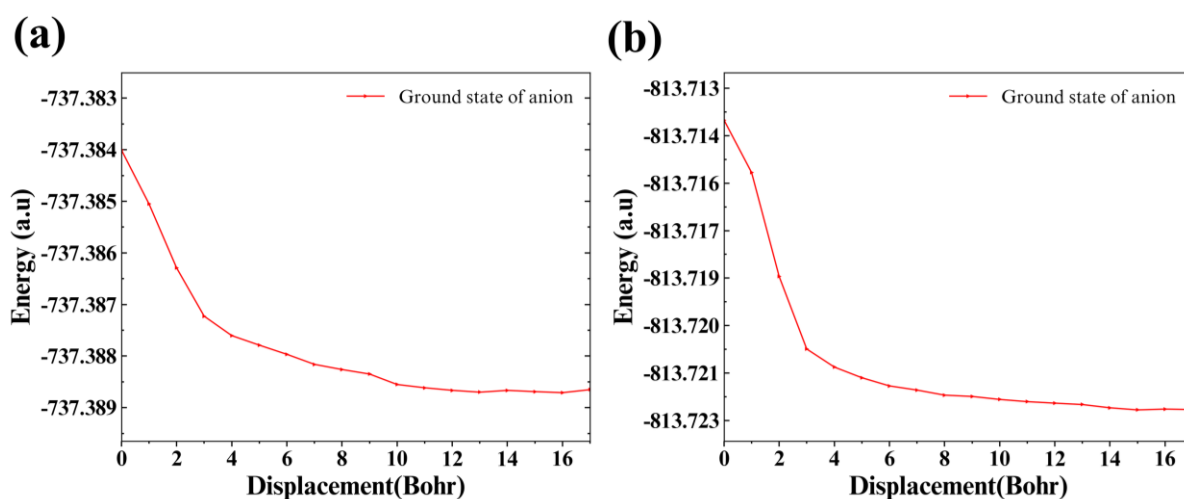


Figure 7. MEP for the proton transfer reaction in (a)Thy-NGly₂ and (b)Thy-ZGly₂.

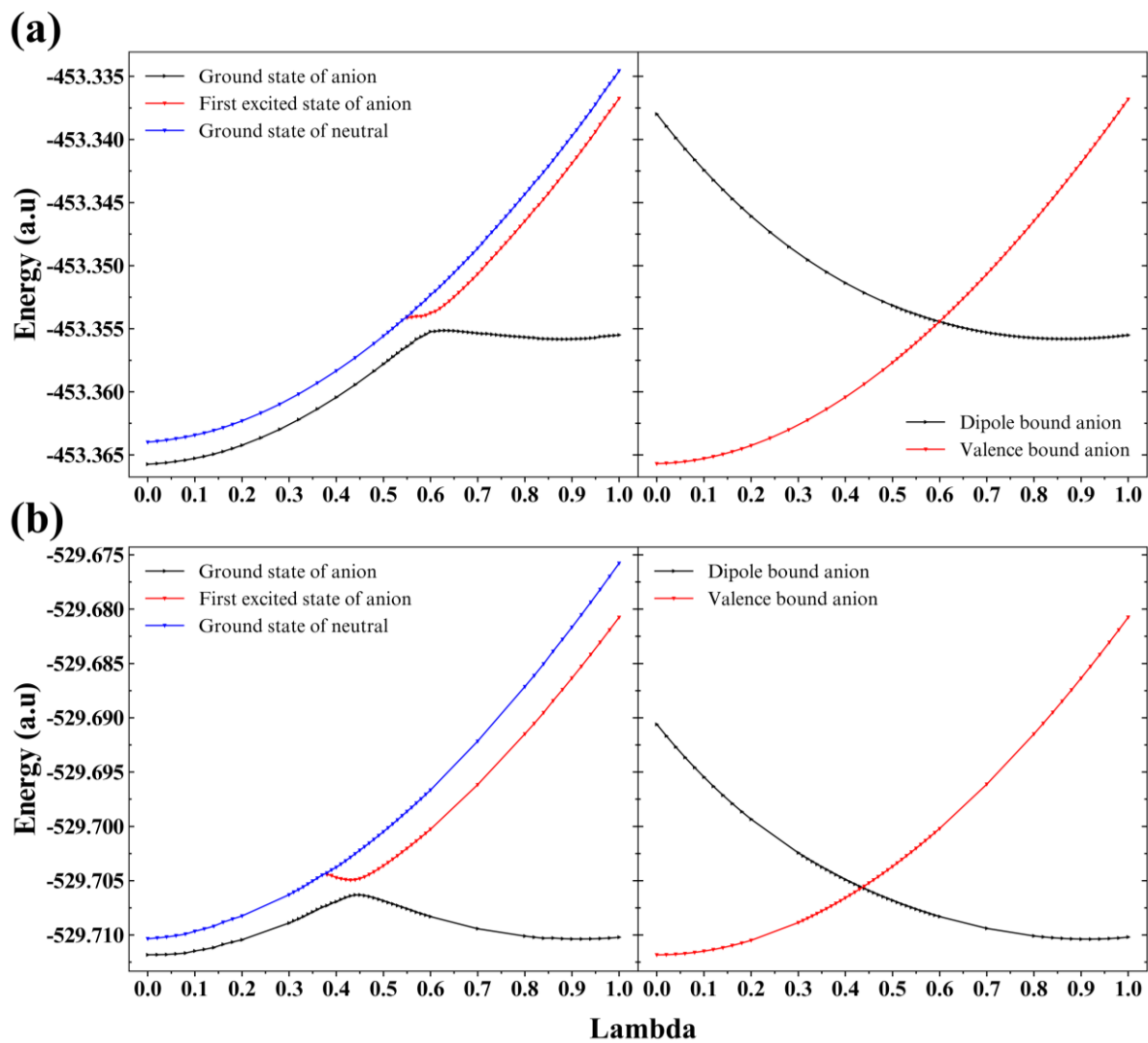


Figure 8. Adiabatic (left) and diabatic (right) PECs for (a) isolated thymine and (b) thymine + water complex.

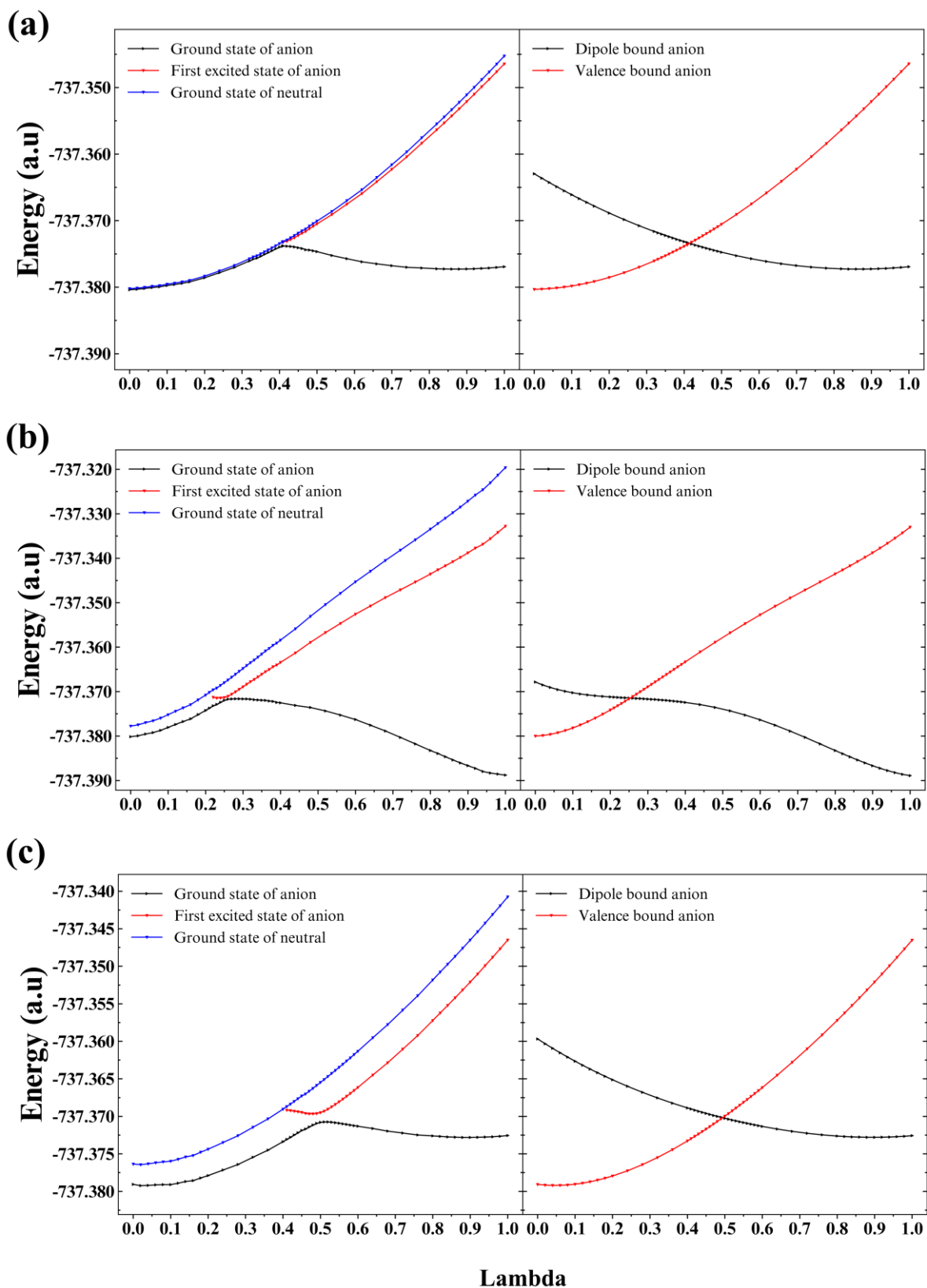


Figure 9. Adiabatic (left) and diabatic (right) PECs for (a) Thy-NGly1, (b) Thy-NGly2, (c) Thy-NGly3.

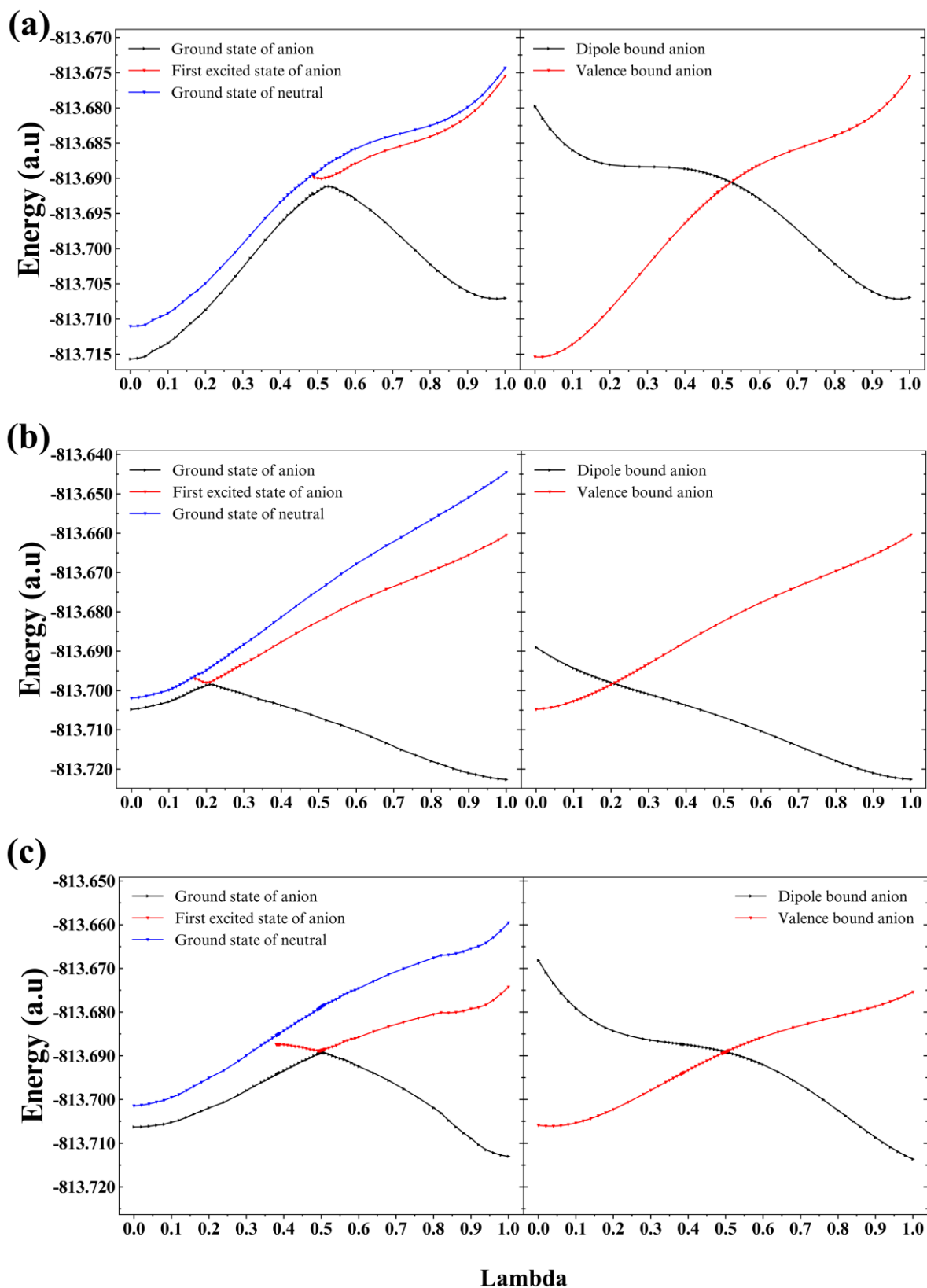


Figure 10. Adiabatic (left) and diabatic (right) PECs for (a) Thy-ZGly1, (b) Thy-ZGly2, (c) Thy-ZGly3.

Table 2. Coupling Constant (meV) and Rate Constant (s^{-1}) of Electron Transfer from the Dipole Bound to Valence Bound State at the EA-EOM-DLPNO-CCSD/aug-cc-pVTZ Level of Theory

Complex	Coupling constant	Rate constant
Thymine	21.68	1.0×10^8
Thymine + Water	18.87	1.8×10^{10}
Thy-NGly1	9.50	8.1×10^9
Thy-NGly2	11.35	4.0×10^{11}
Thy-NGly3	18.14	4.2×10^9
Thy-ZGly1	15.85	1.5×10^7
Thy-ZGly2	7.14	1.2×10^{11}
Thy-ZGly3	4.93	5.1×10^7

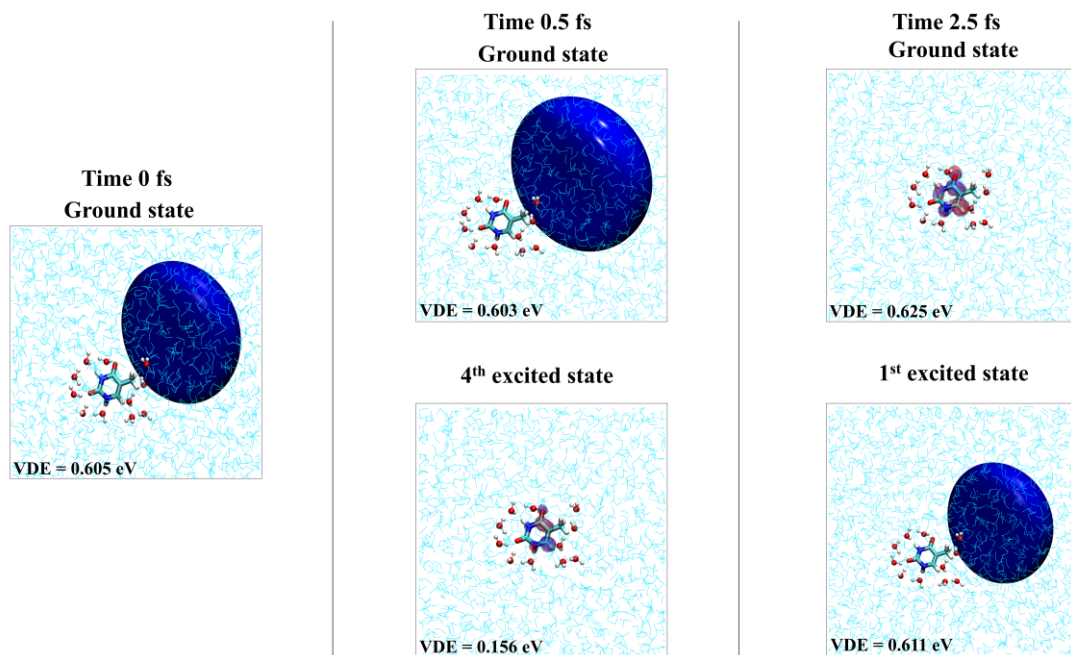


Figure 11. EA-EOM-DLPNO-CCSD dominant transition orbitals depicting the time evolution of anionic state for thymine solvated in water.

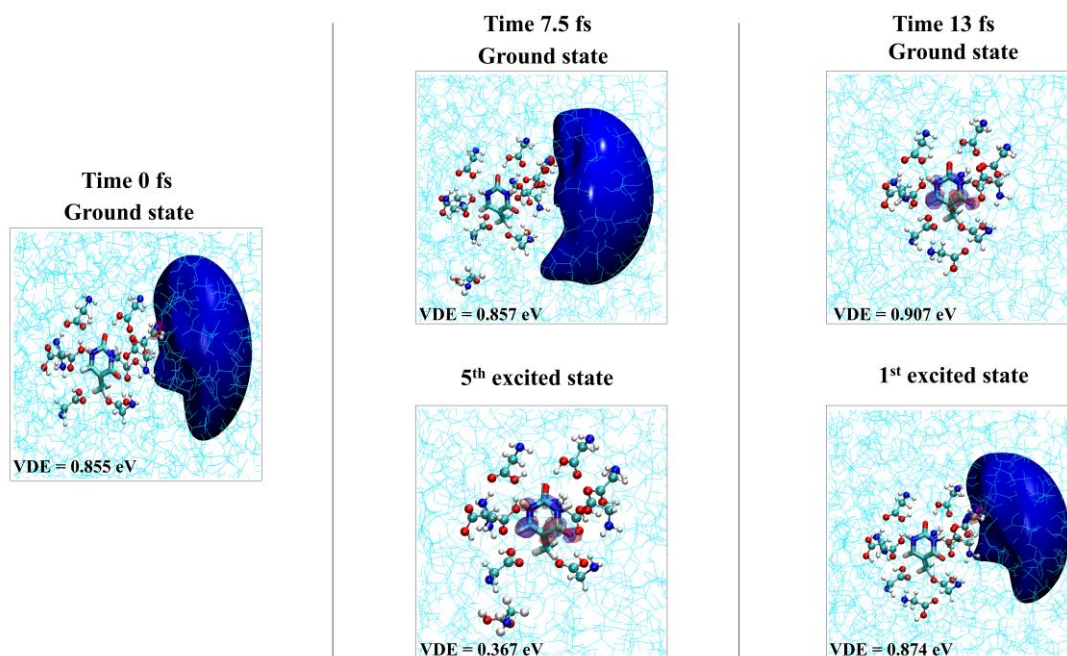


Figure 12. EA-EOM-DLPNO-CCSD dominant transition orbitals depicting the time evolution of anionic state for thymine solvated in native glycine.

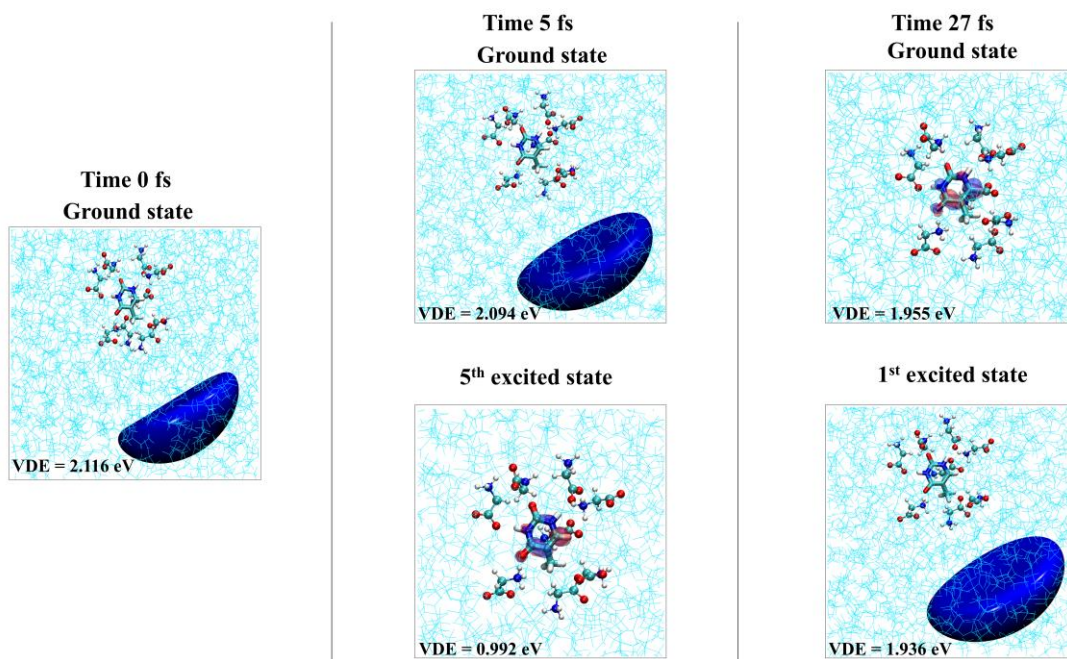


Figure 13. EA-EOM-DLPNO-CCSD dominant transition orbitals depicting the time evolution of anionic state for thymine solvated in zwitterionic glycine.

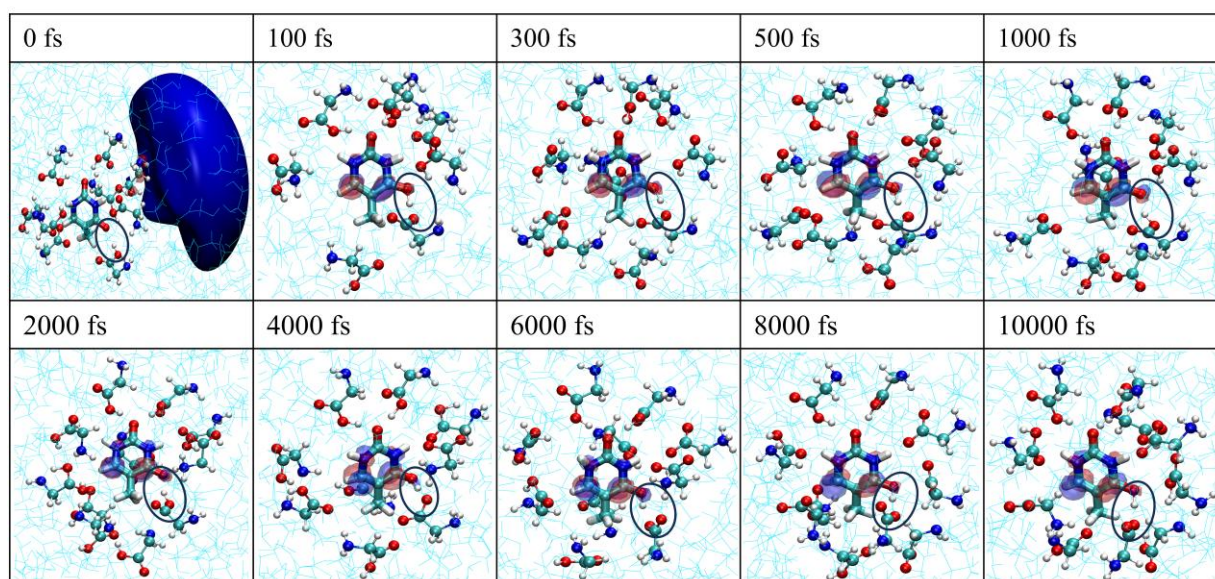


Figure 14. Evolution of the ground-anionic state of thymine in a bulk native glycine environment, illustrating the proton transfer from native glycine to thymine in the first QM/MM trajectory

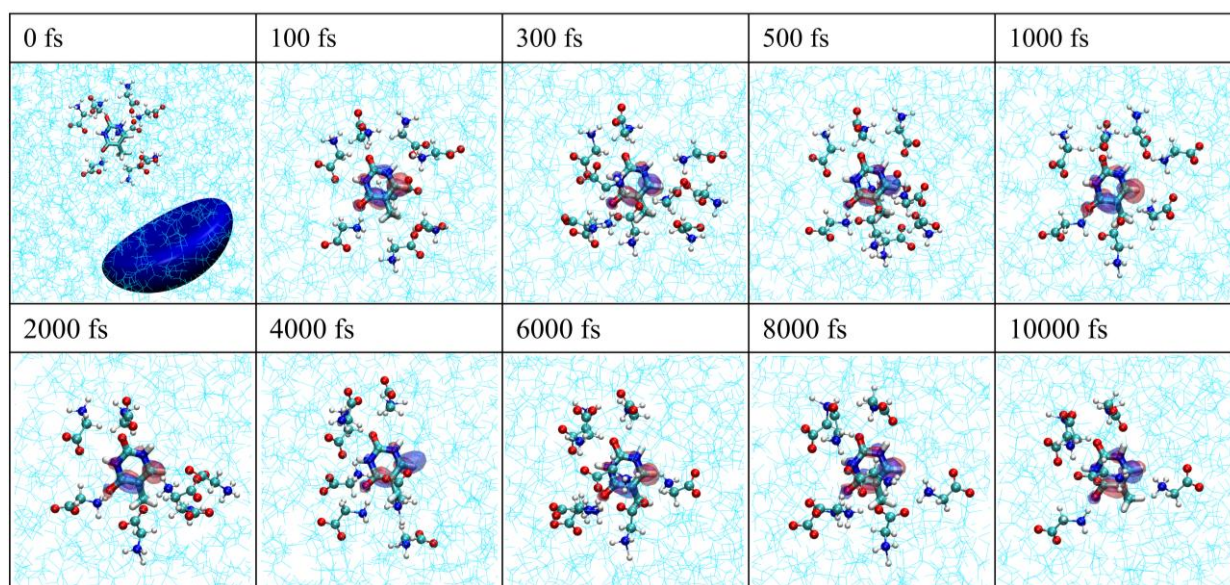


Figure 15. Evolution of the ground anionic state of thymine in a bulk zwitterionic glycine environment in the first QM/MM trajectory.

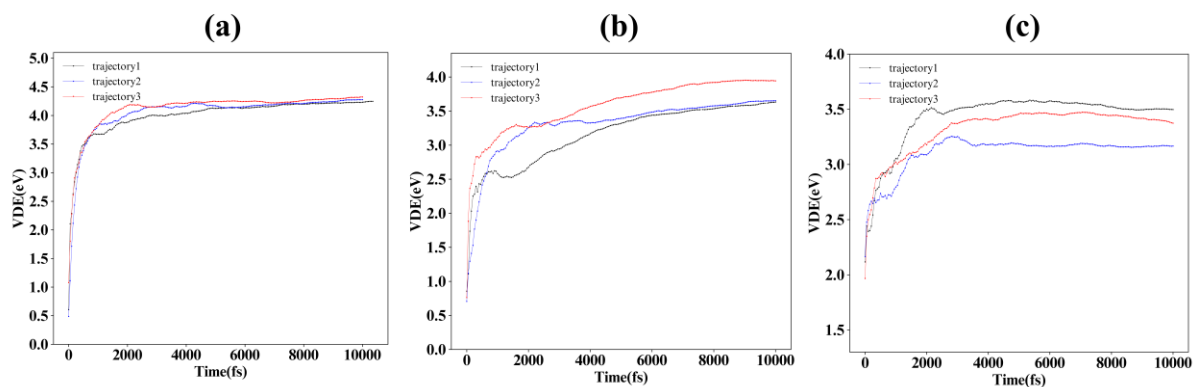


Figure 16. Instantaneous average of the VDE for the ground anionic state of (a) thymine-water (b) thymine-native glycine and (c) thymine-zwitterionic glycine in the QM/MM trajectories.